A New Sol−Gel Route to Aluminum Fluoride Phosphate Glasses: Mechanistic Investigations by NMR Spectroscopy

Long Zhang, Carla C. de Araujo, and Hellmut Eckert*

Institut für Physikalische Chemie, Westfälische Wilhelms-Universität Münster, Corrensstr. 30, D-48149 Münster, Germany

Received January 12, 2005. Revised Manuscript Received April 1, 2005

Homogeneous and transparent sodium aluminum fluoride phosphate gels and glasses were prepared by a novel single-step sol−gel route using aqueous solutions of di-sodium fluorophosphate (Na_2PO_3F) and aluminum lactate ($Al(lact)_3$) as precursors. The structural evolution from the solution to the gel and the final glass is monitored by multinuclear high-resolution liquid and solid-state NMR techniques, providing detailed insight into the reaction mechanism. The ^{19}F NMR results indicate that the covalent F−P bond is stable in these solutions and remains unaffected by the formation of Al−O−P linkages during the polycondensation process from the sol to the gel state. The subsequent annealing at $T > 100$ °C of the xerogel promotes intramolecular fluorine transfer from phosphorus to aluminum, concomitant with the removal of lactate ligands upon heating, resulting in sodium aluminum fluoride phosphate glasses as the final product. In these glasses, all of the fluorine is coordinated to octahedral aluminum ($Al(F,OP)_6$ units), thereby resulting in a significant increase in the Al(VI) concentration compared with the corresponding fluoride-free glasses.

Introduction

Fluoride phosphate glasses have been a subject of increasing interest in the past decade. These glasses form over a wide compositional range and exhibit interesting optical properties, such as low linear and nonlinear refractive indices,[1,2] low phonon energy,[3] a wide spectral transparency (from UV to near-IR),[4] high doping ability with transition metal ions and rare earth ions,[5−7] and tailorable spectroscopic properties by varying the phosphate content.[8] These special optical and physical properties make them promising host materials for applications in photonics, such as optical fiber,[9] optical amplifiers and lasers,[10] frequency upconverters,[11] and optical limiters.[12] Among these glasses, aluminum fluoride phosphate glasses are particularly promising as they combine these optical properties with excellent chemical durability and mechanical properties.[13−16] However, frequently encountered problems associated with standard melt-cooling synthesis procedures are fluoride evaporation loss and crystallization; in addition, shaping possibilities are limited. To overcome these restrictions, alternative preparation routes have been developed, including physical vapor deposition,[17] chemical vapor deposition,[18] electron-beam deposition,[19] and thermal evaporation.[20] However, inherent difficulties of vapor-phase methods arise from the vapor-pressure differences between the precursor species employed, making it hard to control the composition of multicomponent materials. A potential alternative might be the sol−gel approach, which has proven immensely successful for the preparation of amorphous oxide materials.[21] Sol−gel techniques present a number of advantages over traditional glass-making procedures. The molecular-level mixing of the solution precursor

* To whom correspondence should be addressed. Phone 49-251-8329161. Fax: 49-251-8329159. E-mail eckerth@uni-muenster.de.

(1) Weber, M. J.; Layne, C. B.; Saroyan, R. A.; Milam, D. *Opt. Commun.* **1976**, *18*, 171.
(2) Stokowski, S. E.; Martin, W. E.; Yarema, S. M. *J. Non-Cryst. Solids* **1980**, *40*, 481.
(3) Layne, C. B.; Weber, M. J. *Phys. Rev. B* **1977**, *16*, 3259.
(4) Kumar, B. *Mater. Res. Bull.* **1981**, *16*, 179.
(5) Matecki, M.; Jordery, S.; Lucas, J. *J. Mater. Sci. Lett.* **1992**, *11*, 1431.
(6) Matecki, M.; Duhamel, N.; Lucas, J. *J. Non-Cryst. Solids* **1995**, *184*, 273.
(7) Binnemans, K.; Van Deun, R.; Gorller-Walrand, C.; Adam, J. L. *J. Non-Cryst. Solids* **1998**, *238*, 11.
(8) Topfer, T.; Hein, J.; Philipps, J.; Ehrt, D.; Sauerbrey, R. *Appl. Phys. B* **2000**, *71*, 203.
(9) Zuo, X.; Itoh, K.; Toratani, H. *J. Non-Cryst. Solids* **1997**, *215*, 11.
(10) See, for example, (a) Petrov, V.; Griebner, U.; Ehrt, D.; Seeber, W. *Opt. Lett.* **1997**, *22*, 408. (b) Philipps, J.; Topfer, T.; Ebendorff-Heidepriem, H.; Ehrt, D.; Sauerbrey, R. *Appl. Phys. B* **2001**, *72*, 399. Jerez, V. A.; de Araujo, C. B.; Messaddeq, Y.; Ribeiro, S. J. L.; Poulain, M. *J. Appl. Phys.* **2003**, *93*, 1493. (c) Kopf, D.; Kaertner, F. X.; Keller, U.; Weingarten, K. J. *Opt. Lett.* **1995**, *20*, 1169.
(11) See, for example, (a) Adam, J. L.; Duhamel-Henry, N.; Allain, J. Y. *J. Non-Cryst. Solids* **1997**, *213&214*, 245. (b). Poirier, G.; Valdimir, A. J.; de Araujo, C. B.; Messaddeq, Y.; Ribeiro, S. J. L.; Poulain, M. *J. Appl. Phys.* **2003**, *91*, 10221. (c) Philipps, J.; Topfer, T.; Ebendorff-Heidepriem, H.; Ehrt, D.; Sauerbrey, R. *Appl. Phys. B* **2002**, *74*, 233.
(12) Poirier, G.; de Araujo, C. B.; Messaddeq, Y.; Ribeiro, S. J. L.; Poulain, M. *J. Appl. Phys.* **2002**, *91*, 10221.
(13) Matecki, M.; Poulain, M. *J. Non-Cryst. Solids* **1983**, *56*, 111.
(14) Tick, P. A. *J. Am. Ceram. Soc.* **1983**, *66*, 716.
(15) Tick, P. A. *Phys. Chem. Glasses* **1984**, *25*, 149.
(16) Sun, K. H. U.S. Patent 2511225, 1950.
(17) (a) Poignant, H.; Monerie, M.; Baniel, P.; Mercier, A. M.; Jacoboni, C. *Mater. Res. Bull.* **1987**, *22*, 53. (b) Joubert, M. F.; Remillieux, A.; Jacquier, B.; Mugnier, J.; Boulard, B.; Perrot, O.; Jacoboni, C. *J. Non-Cryst. Solids* **1995**, *184*, 341.
(18) (a) Fujiura, K.; Ohishi, Y.; Takahashi, S. *Mater. Sci. Forum* **1991**, *67&68*, 45. (b) Poignant, H.; Mellot, J. L.; Bossis, Y. *Mater. Sci. Forum* **1985**, *5*, 79. (c) Fujiura, K.; Ohishi, Y.; Takahashi, S. *Jpn. J. Appl. Phys.* **1989**, *28*, L147.
(19) Bruce, A. J.; Zydzik, G.; Chui-Sabourin, M. In *Materials Science Forum*; TransTech: Aedermannsdorf, 1991; Vols. 67&68, p 377.
(20) Almeida, R. M.; Morais, P. J. *J. Non-Cryst. Solids* **1995**, *184*, 93.
(21) (a) Brinker, C. J.; Scherer, G. W. *Sol−Gel Science: The Physics and Chemistry of Sol−Gel Processing*; Academic Press: San Diego, 1990. (b) Hench, L. L.; West, J. K. *Chem. Rev.* **1990**, *90*, 33.

10.1021/cm050066z CCC: $30.25
Published on Web 05/11/2005

Table 1. Sample Composition and Precursor Ratios Employed in the Gel Synthesis, Annealing Temperature (T_a) Used for Gel→ Glass Conversion, and Glass Transition (T_g) and Crystallization Temperatures (T_x) of the Annealed Glassy Materials

Na/Al/P/F	$Al(lact)_3$ (mol)	Na_2PO_3F (mol)	H_2PO_3F (mol)	H_3PO_4 (mol)	NaAc (mol)	T_a (±2 °C)	T_g (±10 °C)	T_x (±10 °C)
2:2:1:1	0.004	0.002				350	330	360
2:2:2:1	0.004	0.002		0.002		400	430	470
2:1:2:1	0.004	0.004		0.004		400	420	580
2:2:4:1	0.004	0.002		0.006		400	490	620
2:2:2:2	0.004	0.002	0.002			400	400	440
2:1:2:0	0.004			0.008	0.008	400	450	580
2:2:2:0	0.004			0.004	0.004	400	460	600

species offers the prospect of making very pure and homogeneous materials over a wide range of compositions. In addition, unique applications derive from an included flexibility of shaping (e.g., films, coatings, powders, fibers, monoliths, and gels) and the low processing temperatures used. Despite considerable effort to extend the sol−gel approach to fluoride-containing materials,[22−29] this task has remained a big challenge to the present date. In general, a two-step procedure is employed, involving a preparation of oxide gels, followed by a subsequent fluorination treatment at elevated temperature (near 200−300 °C) in reactive gaseous atmosphere (HF, NH_4F, or NF_3).[22−25] The direct incorporation of fluoride from appropriate solution precursors has only been reported for some ceramic and crystalline systems.[25−29] To take full advantage of the unique features of the sol−gel process in the preparation of fluoride-containing glasses, the development of single-step, low-cost, and nonhazardous procedures is essential. In this contribution, we report the first direct sol−gel preparation route toward aluminum fluoride phosphate gels and glasses. The success of this route is based on the unique chemical reactivity of the precursors di-sodium fluorophosphate and aluminum lactate employed. The structural evolution from sol to gel to glass is monitored by multinuclear single and double resonance NMR spectroscopy, elucidating the mechanisms of gel formation and its structural conversion to the glassy state.

Experimental Section

Materials and Methods. Na−Al−P−O−F gels were prepared from aqueous solutions within a pH range of 2−4, using aluminum lactate (98%, Fluka), di-sodium fluorophosphate (Na_2PO_3F) (98%, Sigma-Aldrich), H_2PO_3F (4 M, freshly prepared from 70% H_2PO_3F solution, Sigma-Aldrich), and H_3PO_4 (1 M) as precursors. H_3PO_4 (1 M) solution was prepared by dissolving solid H_3PO_4 (98%, Fluka) in distilled water. The pH of the mixing solutions was adjusted with nitric acid (1 M, puriss. p.a., Fluka) or ammonia solution (1 M, diluted from concentrated ammonia solution, Aldrich) and controlled within 0.01 units by a pH meter (WTW pH 320, Germany). In a typical preparation, 0.004 mol (1.176 g) of aluminum lactate was dissolved in 10 mL of distilled water, followed by the addition of the appropriate amount of Na_2PO_3F. Samples with different Na/P/F ratios were prepared from Na_2PO_3F as well, adding the required amounts of H_2PO_3F (2 M), H_3PO_4 (1 M), or sodium acetate (NaAc, 99%, Fluka) to reach the compositional balance desired. Table 1 lists the compositions of the samples in the present study and the respective precursors used in each preparation. After stirring the reaction mixture in a plastic beaker for about 20 min, the resulting clear solution was spread onto a flat plastic surface and then gelled in the open air at a temperature between ambient and 50 °C for several days. Upon air-drying, transparent colorless Na−Al−P−O−F xerogels were formed. Usage of NaF, NH_4F, or NH_4HF_2 instead of Na_2PO_3F as the F-precursor always resulted in the formation of opaque gels or crystalline precipitates. Although Na_2PO_3F can in principle be substituted by an appropriate mixture of H_2PO_3F/NaAc, this was not done because the NMR spectra of H_2PO_3F solutions indicate the presence of non-negligible amounts of hazardous HF species. To reduce such hazards, the amount of H_2PO_3F needed in these preparations was kept to the minimum necessary, and only used as a fluorine supplement for the preparation of glasses with F/Na ratios larger than 1/2. Gel annealing was done in glass containers using a Heraeus muffle furnace.

Sample Characterization. Differential thermal analysis (DTA) and thermogravimetric analysis (TGA) were carried out on a NETZSCH STA409 instrument under O_2 atmosphere using a heating rate of 10 K/min. A typical TGA trace is shown in Figure 1a for a xerogel and a glass with composition of Na/Al/P/F = 2:2:4:1, revealing that volatile components (organic residuals and water) are almost completely driven off below 400 °C. Transparent Na−Al−P−O−F glasses were obtained, by heating the xerogels slowly (0.5 °C/min) up to 350−400 °C for several hours in ambient atmosphere. Their noncrystalline state was confirmed by X-ray powder diffraction (Guinier method, Cu $K\alpha_1$ radiation), revealing the typical response of glassy samples. Glass samples annealed at 400 °C show practically no more weight loss due to residual organic constituents. The minor weight loss observed below 200 °C (Figure 1a) arises most likely from surface-adsorbed water. The glass transition (T_g) and crystallization temperatures (T_x) observed from the DTA traces (Figure 1b) are summarized in Table 1. Addition of fluoride into aluminophosphate glass generally tends to decrease the T_g values, consistent with results reported on melt-prepared glasses.[30]

NMR Studies. ^{27}Al and ^{31}P NMR spectra were recorded at resonance frequencies of 130.3 (^{27}Al) and 202.5 MHz (^{31}P) on a

(22) (a) Saad, M.; Poulain, M. *J. Non-Cryst. Solids* **1995**, *184*, 352. (b) Lebullenger, R.; Poulain, M. *J. Non-Cryst. Solids* **1995**, *184*, 166.
(23) (a) Dejneka, M.; Riman, R. E.; Snitzer, E. *J. Am. Ceram. Soc.* **1993**, *76*, 3147. (b) Ballato, J.; Dejneka, R.; Snitzer, E.; Riman, R. E.; Zhou, W. *J. Mater. Res.* **1996**, *11*, 841. (c) Ballato, J.; Riman, R. E.; Snitzer, E. *J. Non-Cryst. Solids* **1997**, *213*, 126.
(24) (a) Konishi, A.; Kanno, R.; Kawamoto, Y. *J. Alloys Compd.* **1996**, *232*, 53. (b) Konishi, A.; Kanno, R.; Kawamoto, Y. *Mater. Res. Bull.* **1995**, *30*, 193.
(25) (a) Fujihara. S.; Ono, S.; Kishiki, Y.; Tada, M.; Kimura, T. *J. Fluorine Chem.* **2000**, *105*, 65. (b) Fujihara. S.; Tada, M.; Kimura, T. *Thin Solid Films* **1997**, *304*, 252. (c) Fujihara. S.; Kato, T.; Kimura, T. *J. Sol-Gel Sci. Technol.* **2003**, *26*, 953.
(26) (a) Rywak, A. A.; Burlitch, J. M. *Chem. Mater.* **1996**, *8*, 60. (b) Duldulao, F. D.; Burlitch, J. M. *Chem. Mater.* **1993**, *5*, 1037. (c) Duldulao, F. D.; Burlitch, J. M. *Chem. Mater.* **1995**, *7*, 2277.
(27) Boyer, D.; Mahiou, R. *Chem. Mater.* **2004**, *16*, 2518.
(28) Zolotar, M. S.; Zavaglia, C. A. C. *J. Non-Cryst. Solids* **1999**, *247*, 50.
(29) Poncelet, O.; Guilment, J.; Martin, D. *J. Sol-Gel Sci. Technol.* **1998**, *13*, 129.
(30) Brow, R. K.; Tallant, D. R.; Osborne, Z. A.; Yang, Y.; Day, D. E. *Phys. Chem. Glasses* **1991**, *32*, 188.

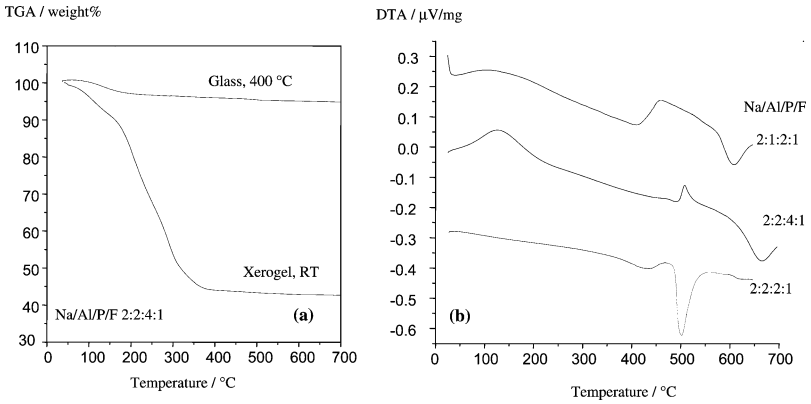

Figure 1. (a) TGA traces of xerogel (formed at 50 °C) and glass (annealed at 400 °C) with composition of Na/Al/P/F 2:2:4:1, obtained at a heating rate of 10 K/min in air. (b) Differential thermal analysis of some representative Na−Al−P−O−F glasses prepared by the sol−gel route. The individual traces have been offset for clarity. The glass transition temperatures T_g and crystallization temperature T_x (onset points) observed are summarized in Table 1.

Bruker DSX-500 spectrometer, using a 4 mm MAS NMR probe. Liquid-state NMR studies were conducted on stationary samples located inside 4 mm zirconia rotors, whereas solid-state NMR data were obtained at MAS rotation frequencies between 10 and 12 kHz. Typical acquisition parameters were pulse length 5.0 μs (90°) for ^{31}P and 1.0 μs (30°) for ^{27}Al, recycle delay 60 s (^{31}P) and 1 s (^{27}Al), respectively. The ^{27}Al and ^{31}P NMR chemical shifts are referenced to 1 M aluminum nitrate aqueous solution and 85% H_3PO_4, respectively. ^{19}F single resonance NMR spectra were acquired at 188.3 MHz in a 4.65 T magnet, using a Bruker DSX400 console. Liquid state ^{19}F NMR studies were conducted on stationary samples located inside 4 mm zirconia rotors, whereas for solid state ^{19}F MAS NMR spectra a 2.5 mm probe operated at a MAS frequency of 25 kHz was used. The faster spinning is essential to remove homonuclear ^{19}F−^{19}F dipolar broadening and to separate the central MAS signals from spinning sidebands more effectively. To suppress ^{19}F background signals, a rotor-synchronized spin−echo (90° − 0.04 ms −180° − 0.04 ms − acq) pulse sequence with an XY-4 phase cycle[31] was used. The 90° pulse length in these measurements was 2.5 μs. A total of 320−1024 scans were acquired with a relaxation delay of 10 s. Experiments using longer relaxation delays (up to 100 s) were conducted to ensure that the spectra obtained under the above-reported conditions yielded representative results. Chemical shifts are externally referenced to $CFCl_3$.

To probe for the presence and strength of the heteronuclear dipole−dipole couplings, the rotational echo double resonance (REDOR)[31−33] and rotational echo adiabatic passage double resonance (REAPDOR)[34,35] techniques were used. The heterodipolar coupling between the nuclear spin species *S* (whose signal is detected) and spatially close nuclear species *I* is normally averaged out by MAS; in *S*{*I*} REDOR (REAPDOR), this interaction is reintroduced, however, by applying π-pulses (adiabatic mixing pulses) on the *I* channel in the middle of the rotor period. As a result, the *S*-spin signal intensity is diminished relative to a reference experiment without *I*-spin irradiation (intensity S_0) if heterodipolar couplings are present. The magnitude $(S_0 - S)/S_0$ of the normalized difference signal depends on both the strength of the dipole−dipole coupling and the length NT_r (number of rotor cycles times duration of one rotor period) of the overall dipolar evolution time. Table 2 summarizes the specific conditions used in the various REDOR and REAPDOR measurements conducted in the present study.

Table 2. Experimental Conditions Used in the Double Resonance NMR Experiments

combination	$\nu_0(S)^a$ (MHz)	$\nu_0(I)^b$ (MHz)	$\tau_{90°}(S)^c$ (μs)	$\tau_{90°}(I)^d$ (μs)	$\tau_a(I)^e$ (μs)	T_1^f (s)	NS[g]
^{27}Al{^{19}F} REDOR	104.3	376.6	2.5	2.5		2	128−512
^{27}Al{^{31}P} REDOR	130.3	202.5	3.0	3.0		2	256
^{19}F{^{31}P} REDOR	376.6	162.5	2.5	3.0		10	128−256
^{19}F{^{27}Al} REAPDOR	376.6	104.3	2.5	4.0	20	10	128−256
^{19}F{^{23}Na} REAPDOR	376.6	105.3	2.5	4.0	20	10	128−256

[a] *S*-spin resonance frequency. [b] *I*-spin resonance frequency. [c] *S*-spin-90° pulse length. [d] *I*-spin-90° pulse length. [e] Adiabatic passage mixing time in REAPDOR. [f] Relaxation delay. [g] Number of scans.

^{27}Al{^{31}P} REDOR experiments were conducted in a 4 mm Bruker ^{31}P−X double resonance probe in a 11.7 T magnet while all the REDOR experiments involving ^{19}F nuclei utilized a 4 mm Bruker triple resonance probe in a 9.4 T magnet. All of the double resonance measurements were carried out at the spinning frequency of 15 kHz.

Results, Assignment, and Interpretation

Structural Evolution. To gain insight into the structural evolution during the sol → gel → glass conversion, ^{19}F, ^{27}Al, and ^{31}P NMR spectra were recorded at the various processing steps. Figure 2 summarizes the results for Na/Al/P/F 2:2:2:1 samples prepared from $Al(lact)_3/Na_2PO_3F/H_3PO_4$ mixtures. The ^{19}F and ^{31}P spectra of Na_2PO_3F solution show simple doublets characterized by $\delta(^{19}F) = -75$ ppm, $\delta(^{31}P) = 0.8$ ppm, and $^1J(^{19}F-^{31}P) = 886$ Hz (see Figure 2a and b). Figure 2c reveals that the F−P bond remains intact in solution upon addition of $Al(lact)_3$ and H_3PO_4. Only the weak signal near −160 ppm (Figure 2c) can be attributed to the formation of a small amount of Al-bound fluoride species. The ^{27}Al (Figure 2e) and ^{31}P (Figure 2d) spectra of these mixtures can be understood in terms of the analogous fluoride-free solutions:[36] in particular, the complicated ^{27}Al NMR spectra reflect a multitude of coordination complexes with mixed ligation of lactate, water, and phosphate, $[Al(lact)_{3-x}(H_2O)_{2x-y}(PO_3)_y]^{x-y}$ ($0 \le x \le 3$, $0 \le y \le 2x$), as discussed previously.[36] The ^{31}P NMR spectra reveal the

(31) Gullion, T. *Magn. Reson. Rev.* **1997**, *17*, 83.
(32) Gullion, T.; Schaefer, J. *J. Magn. Reson.* **1989**, *81*, 196.
(33) Bertmer, M., Eckert, H. *Solid State Nucl. Magn. Reson.* **1999**, *15*, 139.
(34) Gullion, T. *J. Magn. Reson. A* **1995**, *117*, 326.
(35) Chopin, L.; Vega, S.; Gullion, T. *J. Am. Chem. Soc.* **1998**, *120*, 4406.
(36) Zhang, L.; Eckert, H. *J. Mater. Chem.* **2004**, *14*, 1605.

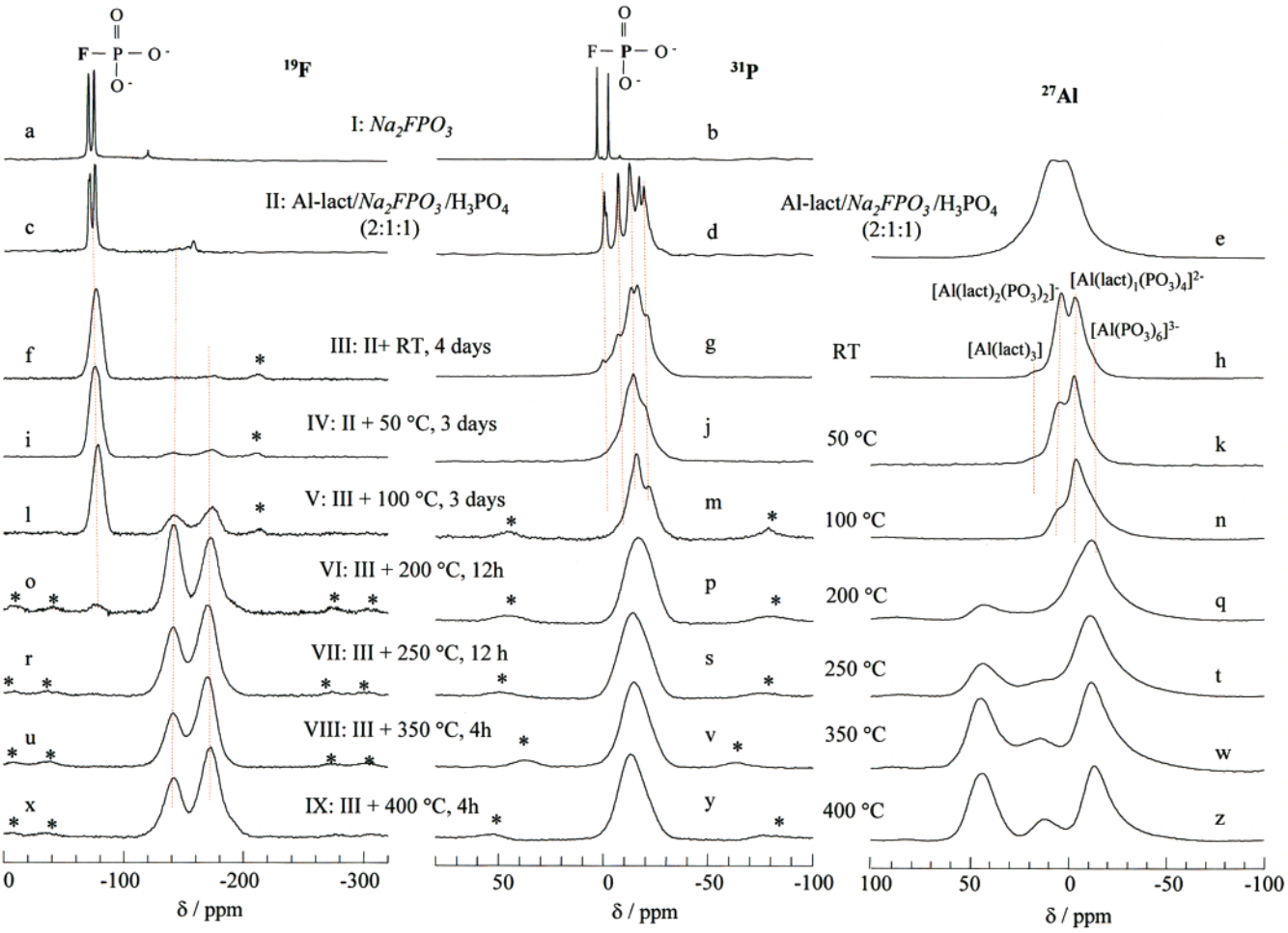

Figure 2. 188.3 MHz ^{19}F (left), 202.5 MHz^{31}P (middle), and 130.3 MHz ^{27}Al (right) NMR spectra of the Na−Al−P−O−F samples (Na/Al/P/F = 2:2:2:1), at various processing stages from the sol to gel to glass conversions. The parts a−e are solution state NMR spectra, while parts f−z were obtained under MAS conditions. Vertical lines denote the chemical shifts of various species identified. Spinning sidebands are indicated with asterisks.

presence of orthophosphate (both F-free and F-bound) species bound to zero (Q^0_0, 0 ppm), one (Q^0_1, −7 ppm), two (Q^0_2, −12 ppm), and three (Q^0_3, −17 ppm) aluminum atoms.

Upon air-drying the sols at temperatures ranging from ambient to 50 °C for several days, transparent colorless xerogels are formed. The ^{19}F MAS NMR spectra of these materials (Figure 2f and i) are still dominated by the F−P(O)O_2^{2-} species at −75 ppm; in addition, weak peaks at −140 and −170 ppm are observed. We attribute the latter resonances to Al-bound species, as discussed in more detail below. With increasing the gel-processing and annealing temperature, the concentrations of these Al-bound species increase, while the F−P(O)O_2^{2-} species disappear successively. The most dramatic changes occur within the temperature range between 100 °C and 200 °C. In samples annealed above 250 °C (Figure 2r, u, and x), the −75 ppm signal is absent, indicating that the F−P bonds have completely disappeared.

The ^{31}P NMR spectra of the xerogels (Figure 2g) can be easily understood based on the solution-state spectra (note the close resemblance of Figure 2d and g).[36] With increasing the processing temperature from ambient to 100 °C (Figure 2g, j, and m), the center of gravity of the signal shifts monotonically toward lower frequency, reflecting a further gradual increase of P/Al connectivity. The structural evolution of phosphorus upon further heating above 200 °C involves the replacement of P−F bonds by P−(OAl)− and P−(ONa) linkages in the final glass. The average ^{31}P chemical shift of −12 ppm suggests that Q^0_2 units make a dominant contribution.

Based on the conclusion from ^{19}F NMR that virtually no F−Al bonds exist in xerogels formed up to 50 °C (see Figure 2f and i), the four ^{27}Al resonances observed in these xerogels (Figure 2h and k) can be assigned as usual to octahedral aluminum species with mixed lactate and phosphate ligands, i.e., $[Al(lact)_2(PO_3)_2]^-$ (18 ppm), $[Al(lact)_3]$ (6 ppm), $[Al(lact)(PO_3)_4]^{2-}$ (−4 ppm), and $[Al(PO_3)_3]^{3-}$ (−13 ppm), respectively.[36] With increasing the processing temperature (Figure 2h, k, and n), the lactate groups linked to aluminum are gradually replaced by phosphorus and/or fluorine ligands, resulting in significant low-frequency signal displacements. Gel annealing at 200 °C produces a new ^{27}Al resonance near 45 ppm (Figure 2q), which is well-known in aluminophosphate glasses and has been assigned to a polymerized $Al(OP)_4$ unit.[37−40] Indeed, ^{27}Al{^{31}P} as well as ^{27}Al{^{19}F} REDOR conducted on these samples confirm that all of the

(37) Lang, D. P.; Alam, T. M.; Bencoe, D. N. *Chem. Mater.* **2001**, *13*, 420.
(38) Egan, J. M.; Wenslow, R. M.; Mueller, K. T. *J. Non-Cryst. Solids* **2000**, *261*, 115.
(39) Brow, R. K.; Kirkpatrick, R. J.; Turner, G. L. *J. Am. Ceram. Soc.* **1993**, *76*, 919.
(40) Zhang, L.; Eckert, H. *Solid State Nucl. Magn. Reson.* **2004**, *26*, 132.

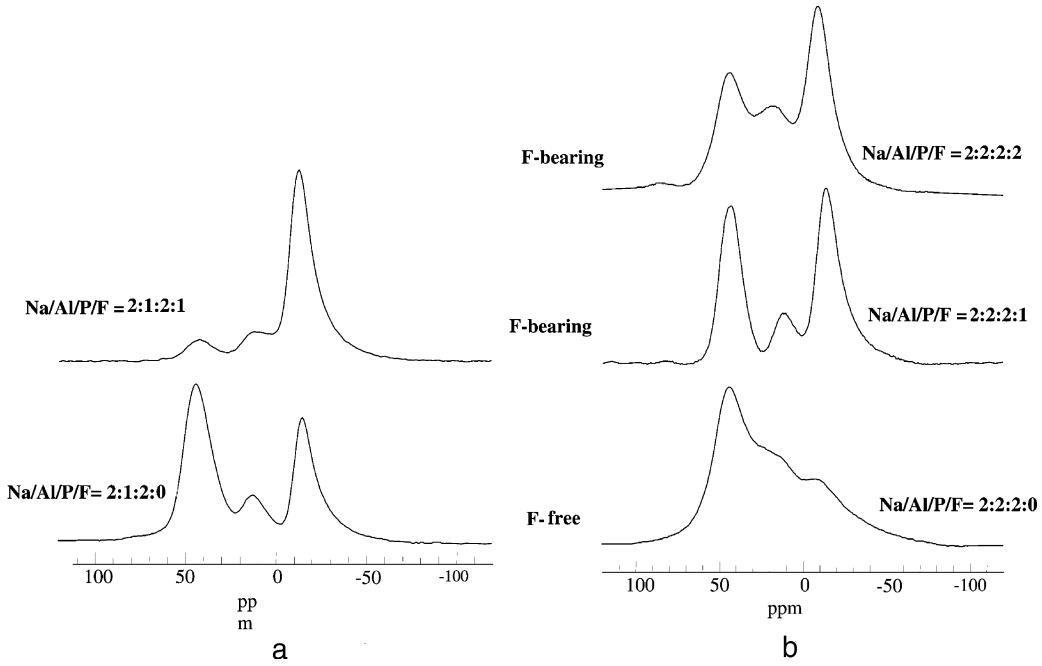

Figure 3. 130.3 MHz ^{27}Al MAS NMR spectra of Na−Al−P−O−F glass with Na/Al/P/F 2:1:2:*x* (left) and 2:2:2:*x* (right). Note that the concentration of octahedral aluminum sites increases significantly with increasing fluorine content.

four next-nearest neighbors are phosphorus (see next section). The concentration of these Al(IV) sites increases further following the subsequent processing at higher temperatures. Following annealing at 250 °C (Figure 2t), the lactate-linked aluminum species are no longer detectable, whereas the well-resolved signals around 45, 15, and −13 ppm, which are typical of Al(IV), Al(V), and Al(VI) environments in aluminophosphate glasses, are now observed.

Effect of Fluoride on the Structure of Aluminophosphate Glass. After annealing the Na−Al−P−O−F xerogels at 350−400 °C, transparent glasses were obtained. To illustrate the structural role of the fluorine atoms incorporated into the aluminophosphate glass network, Figure 3 compares the ^{27}Al NMR spectra of both Na−Al−P−O−F glasses and corresponding F-free aluminophosphate glasses with composition of Na/Al/P/F = 2:1:2:*x* (Figure 3a) and 2:2:2:*x* (Figure 3b) (for F-free glass, $x = 0$). Clearly, the presence of fluorine results in a significant increase in the relative concentration of Al(VI) units, which increases proportionally with *x* (see Figure 3b). We believe this effect to arise from ligation of fluorine to octahedral aluminum, resulting in mixed Al(F,OP)$_6$ local environments.

To support this hypothesis, Figure 4a shows the ^{27}Al{^{19}F} REDOR results of the representative Na−Al−P−O−F glass with composition Na/Al/P/F ratio 2:2:2:1. Clearly, the signals attributed to Al(VI) units are significantly attenuated by ^{19}F irradiation, indicating that fluorine atoms are in close proximity of these units. In contrast, the 45 ppm resonance assigned to Al(IV) species is virtually unaffected by the ^{19}F irradiation, suggesting that these units are remote from fluorine atoms. Thus, the incorporated fluorine is almost entirely coordinated to octahedral aluminum units (a small amount of fluorine might also be ligated to pentahedral units). These results are supported by complementary ^{27}Al{^{31}P} REDOR experiments (see Supporting Information Figure S1). While in a sodium aluminophosphate glass with composition of Na/Al/P = 2:1:2, the local environment of each aluminum unit is entirely dominated by phosphorus ligation;[39,40] in the corresponding Na/Al/P/F = 2:1:2:1 glass the magnetic dipole−dipole coupling between the ^{27}Al(IV) and ^{31}P remains unchanged, while that between ^{27}Al(VI) and ^{31}P is significantly diminished, reflecting a reduction in the number of Al−O−P linkages. This comparison reveals that the Al(OP)$_6$ environment present in the F-free glass has been changed into a mixed Al(OP, F)$_6$ environment in the fluoride-containing glass.

To facilitate the assignments of the ^{19}F NMR signals at −140 and −170 ppm observed in the single-pulse experiments, heterodipolar interactions between ^{19}F and ^{23}Na, ^{27}Al, and ^{31}P were probed by REDOR or REAPDOR experiments. Typical results obtained on a sample with Na/Al/P/F 2:2:2:1 are summarized in Figure 4b−d. In each part of the figure, the upper trace represents the ^{19}F single resonance spin−echo signal, whereas the bottom trace shows the signal acquired following irradiation of the respective heteronuclei in the middle of the rotor period. Significant signal attenuation observed in the latter experiment indicates the presence of substantial dipolar couplings, revealing connectivity or spatial proximity. The ^{19}F{^{27}Al}REAPDOR (Figure 4b) experiment indicates that the fluorine species resonating at −140 ppm interacts with aluminum more strongly than that giving rise to the −170 ppm signal. The opposite effect is observed with respect to the interaction with ^{23}Na (^{19}F{^{23}Na} REAPDOR, Figure 4c). These results suggest that the ^{19}F signals at −140 and −170 ppm might be attributed to bridging (Al−F−Al) and nonbridging (Al−F···Na$^+$) fluorine species, respectively. This idea is further supported by the ^{19}F{^{31}P} REDOR experiments conducted on these samples. As seen from Figure 4d, the ^{31}P irradiation causes an obvious attenuation of both ^{19}F signals at −140 and −170 ppm; however, the effect is more pronounced for the −140 ppm resonance. As no more P−F bonds exist in these samples

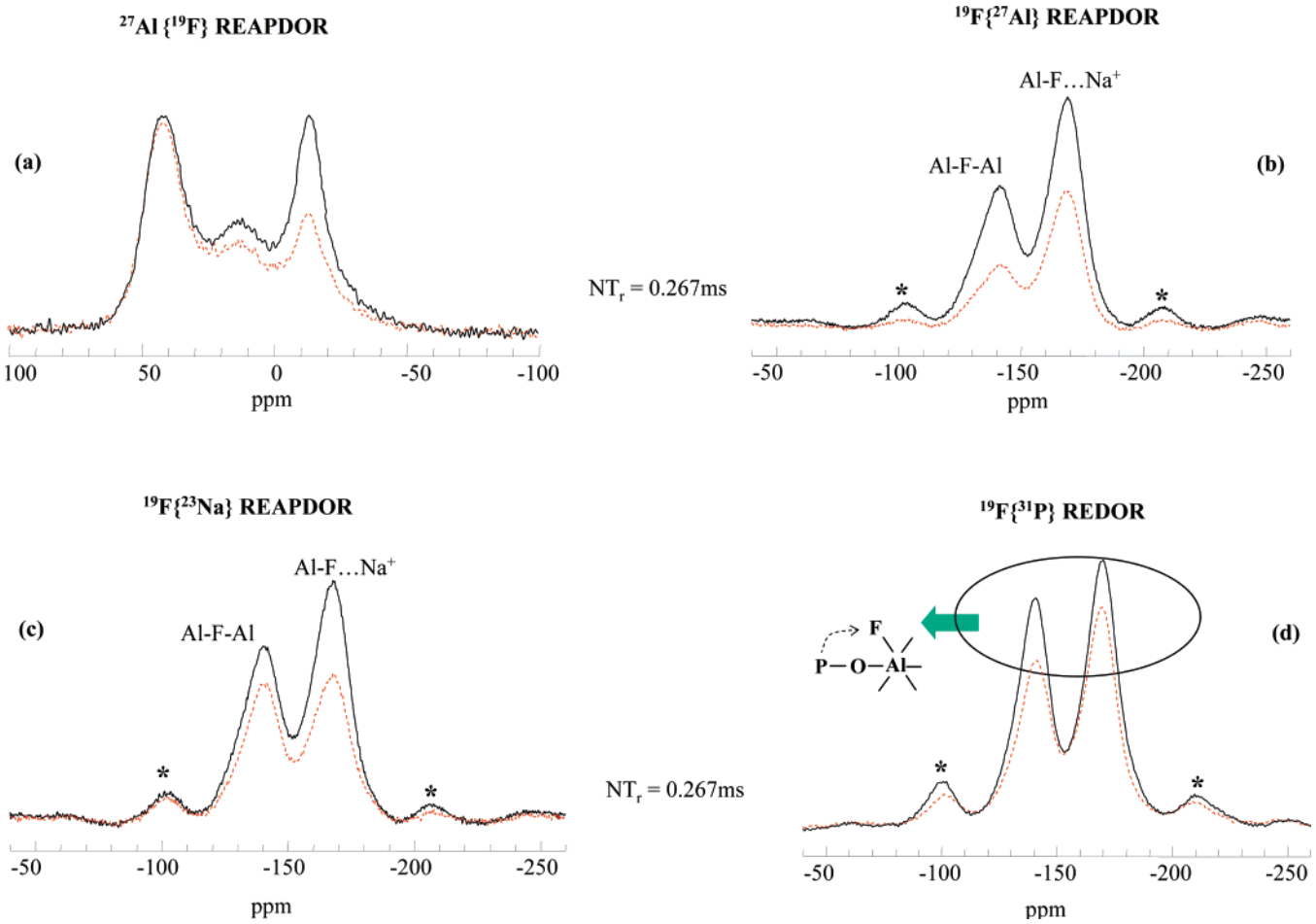

Figure 4. Double resonance NMR studies carried out on the glass with Na/Al/P/F 2:2:2:1: (a) ^{27}Al {^{19}F}REDOR; (b) ^{19}F{^{27}Al} REAPDOR; (c) ^{19}F{^{23}Na} REAPDOR; (d)^{19}F{^{31}P} REDOR. In each individual trace, the upper and bottom curves represent the observe-nuclei signals without and with irradiation of the respective heteronuclei during the evolution period of 0.267 ms, respectively. Spinning sidebands are indicated with asterisks.

(absence of peak near −75 ppm), the ^{19}F{^{31}P} REDOR attenuation must arise from dipolar coupling to phosphate species completing the octahedral aluminum coordination environment. Consistent with the assignment of the ^{19}F resonances, a larger difference signal is expected for the bridging fluoride species. Finally, the signal attenuations of both fluorine signals by ^{31}P irradiation in ^{19}F{^{31}P} REDOR experiments indicate that the fluorine is homogeneously distributed over the Al(VI) sites of the Al−O−P network and no AlF_3-like islands are formed.

Discussion and Conclusions

The results of the present study give important mechanistic insights into the formation of gels and glasses in the $Al(lact)_3/Na_2PO_3F$ system. We previously discussed the molecular mechanism of gel formation in the $Al(lact)_3/H_3PO_4$ sol−gel system,[36] which involves the reaction of mixed aluminum lactate hydrate complexes, $[Al(lact)_{3-x}(H_2O)_{2x}]^{x+}$, with the phosphate species. In the $Al(lact)_3/Na_2PO_3F$ sol−gel system, the ^{19}F NMR spectra reveal that the overwhelming majority of the fluorine atoms remain covalently bound to phosphorus as $F-P(O)O_2^{2-}$ species during the polymerization process. Thus, the reactions can be summarized by the scheme given in Figure 5a.

During the course of the sol−gel conversion, the continuous progress of these reactions promotes further removal of H_2O and lactate from the aluminum coordination sphere by F-bound phosphorus ligands, building larger and larger units and ultimately resulting in the formation of polymeric gel in which aluminum, phosphorus, and fluorine establish multiple −(F)P−O−Al− linkages. The key features of the present sol−gel route, resulting in the successful preparation of transparent Na−Al−P−O−F gels and glasses, are as follows: (a) the peculiar chelation properties of aluminum lactate in aqueous solution, which forms the basis of its reactivity with phosphate, and (b) the stability of the F−P bond under polymerization conditions, circumventing the rapid precipitation of aluminum fluoride from such solutions. Based on the work reported here, the structure of the xerogel can be schematically depicted by Figure 5b.

Upon heating of the xerogels, the successive removal of lactate residues from the aluminum coordination sphere happens concurrently with the transfer of P-bound fluorine to the aluminum species nearby, resulting in the dramatic structural changes evident in Figure 2l−q. After heating at 200 °C, virtually all of the fluorine in the sample is aluminum-bound and no more P−F bonds exist (Figure 2o). Further heating to 400 °C results in the formation of a Na−Al−P−O−F glass network established on the basis of polymerized $Al(OP)_4$, $Al(OP)_5$, $Al(F,OP)_6$, and tetrahedral phosphate units, as schematically illustrated in Figure 5c. Since all the fluorine is incorporated into the coordination

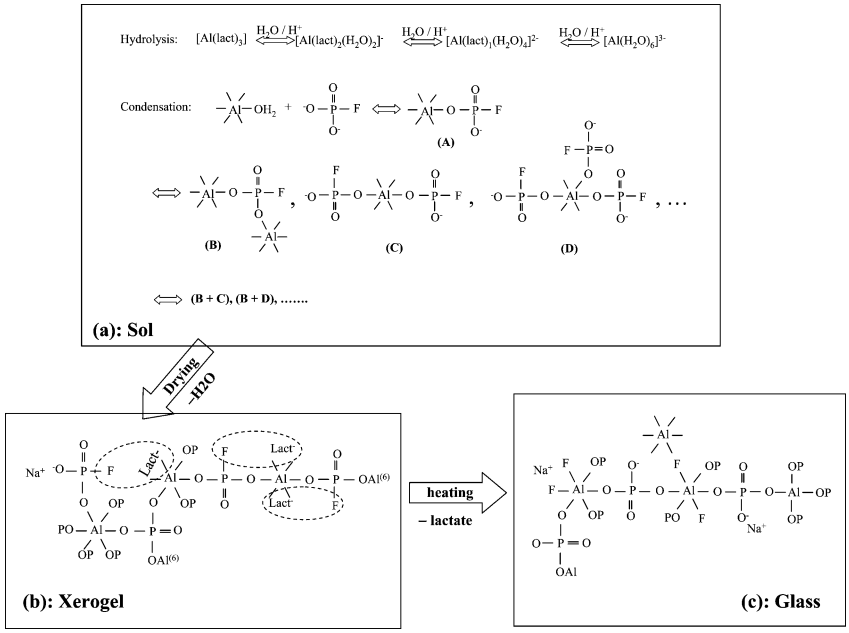

Figure 5. Scheme illustrating the structural evolution in the Na−Al−P−O−F system: (a) sol; (b) xerogel; (c) glass.

sphere of Al(VI) units, Na−Al−P−O−F glasses contain a higher fraction of octahedral aluminum than the corresponding fluorine-free materials (Figure 3).

In summary, we have developed a novel sol−gel route based on di-sodium fluorophosphate and aluminum lactate solution to directly incorporate fluorine into aluminophosphate-based materials, resulting in homogeneous and transparent gels and glasses. The route from the solution to the gel and the final glass was monitored by high-resolution liquid-state NMR and advanced solid-state NMR techniques, elucidating the molecular mechanism and the nature of fluorine incorporation into these materials.

To our knowledge, the present contribution reports the first successful preparation of fluoride-containing gels and glasses via a direct fluoride-incorporated sol−gel route, and the first sol−gel synthesis in which Na_2PO_3F has been used as a precursor. Compared with the previously reported procedures (gaseous fluorination treatment of oxide polymeric gels), the present sol−gel route exhibits some attractive advantages by simplifying the process, eliminating potentially hazardous fluorination agents, and offering the prospect of forming more homogeneous products. Future studies will be devoted to the preparation and application of thin films and to the detailed structural characterization of the glasses as a function of elemental composition.

Acknowledgment. Financial support from Deutsche Forschungsgemeinschaft (grant Ec168/4-1) is gratefully acknowledged. C.C. de Araujo thanks the NRW Graduate School of Chemistry for a personal stipend. We thank Ms. Wilma Pröbsting for the thermoanalytical characterization.

Supporting Information Available: Supplemental figure showing $^{27}Al\{^{31}P\}$ REDOR of F-bearing (Na/Al/P/F = 2:1:2:1) and F-free (Na/Al/P 2:1:2) glasses (PDF). This material is available free of charge via the Internet at http://pubs.acs.org.

CM050066Z